Achieving extraordinary structural efficiency in a wrought magnesium rare earth alloy

S. K. Panigrahi, R. S. Mishra, R. C. Brennan & K. Cho

View supplementary material

Published online: 29 Jan 2020.

Submit your article to this journal

View related articles

View Crossmark data

MATERIALS RESEARCH LETTERS

Taylor & Francis
Taylor & Francis Group

ORIGINAL REPORT

🔓 OPEN ACCESS   Check for updates

Achieving extraordinary structural efficiency in a wrought magnesium rare earth alloy

S. K. Panigrahi[a], R. S. Mishra [b], R. C. Brennan[c] and K. Cho[c]

[a]Department of Mechanical Engineering, Indian Institute of Technology Madras, Chennai, India; [b]Centre for Friction Stir Processing, Department of Materials Science and Engineering, University of North Texas, Denton, TX, USA; [c]U.S. Army Research Laboratory, Aberdeen Proving Grounds, MD, USA

ABSTRACT

The opportunities for wrought magnesium products in a wide range of structural and functional materials for transportation, energy generation, energy storage and propulsion are increasing due to their light-weighting benefits, high specific strength and ease of recyclability. However, the current uses of wrought magnesium alloys for structural applications are limited due to comparatively low strength, high yield strength asymmetry and poor formability & superplasticity. In the present work, we developed an ultrafine-grained magnesium alloy with an extraordinary strength and ductility combination, exceptional high specific strength, zero yield strength asymmetry and excellent high strain rate superplasticity.
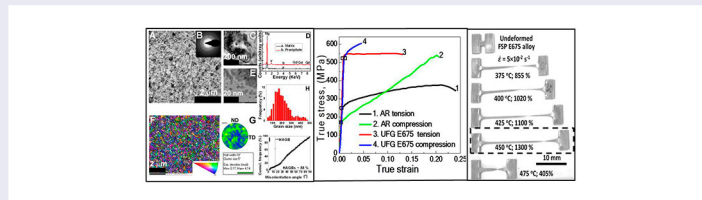
IMPACT STATEMENT

We have developed friction stir processed UFG microstructure in a rare-earth containing magnesium alloy and achieved exceptional strength-ductility combination along with no yield asymmetry and extraordinary high strain rate superplasticity.

1. Introduction

In the view of compelling needs for economical usage of scarce energy resources and ever-stricter control over emissions to lower environmental impact, automotive and aerospace industries are searching for alternative advanced light-weight structural materials to the existing conventional materials [1,2]. Being the lightest and energy-efficient structural material, magnesium (Mg) alloys offer a strong potential in this regard. Mg alloys are the right candidate materials to replace steel and aluminum alloys in automotive and aerospace components since its density is two-third of aluminum and one-quarter of steel [1]. However, the application of Mg alloys in structural field is limited due to their moderate/low

strength, poor ductility, yield strength asymmetry and lack of high strain rate superplasticity.

In this paper, we report a strategy to simultaneously improve strength, ductility and high strain rate superplasticity (HSRS) with elimination of yield strength asymmetry. By engineering nano-precipitates and thermally stable ultrafine intermetallic compounds in an ultrafine-grained (UFG) magnesium rare earth (Mg-RE) alloy, we were able to achieve the highest combination of strength-ductility and highest HSRS among all the existing Mg alloys reported in the literature till date [3–43]. Along with this, the tension-compression yield asymmetry was eliminated. The objectives of the present work were two-fold. The first objective was to develop a

---

strategy to produce unique microstructure in the present alloy in order to achieve the above-mentioned combination of properties. The second objective was to establish the fundamental insight into the governing mechanisms for achieving such extraordinary properties.

2. Materials and methods

A Mg-6Y-7Gd-0.5Zr (in wt.%) wrought alloy (E675) was used for this study. The E675 alloy was subjected to a combined process of three-pass friction stir processing (FSP) and ageing treatment to develop UFG microstructure with hierarchical (fine and coarse) precipitates. First two FSP passes were carried out with high heat input for solutionization and grain refinement. The third FSP pass was carried out with low heat input for texture randomization and further microstructural refinement. The nano-precipitates were dispersed into the UFG matrix by proper aging treatment of 65 h at 180°C to achieve high strength and HSRS. Hereafter, this precipitate contained UFG alloy will be referred as UFG E675 alloy.

The detailed experimental procedures for characterization of the developed UFG E675 alloy are provided in the supplementary file.

3. Results and discussion

3.1. Microstructural characterization

The microstructure and texture of the UFG E675 alloy were characterized by transmission electron microscopy (TEM) and electron backscattered diffraction (EBSD) analysis, respectively. Figure 1(A) is a bright field TEM image of the present alloy which shows dislocation free, well defined equiaxed ultrafine grains. The ring-type diffraction pattern (Figure 1(B) indicates that the grain boundaries are mostly high angle type and the distribution of matrix grains are relatively random. A lot of cuboid/spherical shaped phases with a mean diameter of 75 ± 60 nm are also observed at grain boundaries and grain interior (Figure 1(C)). The corresponding EDS patterns (Figure 1(D)) indicate that they are rich
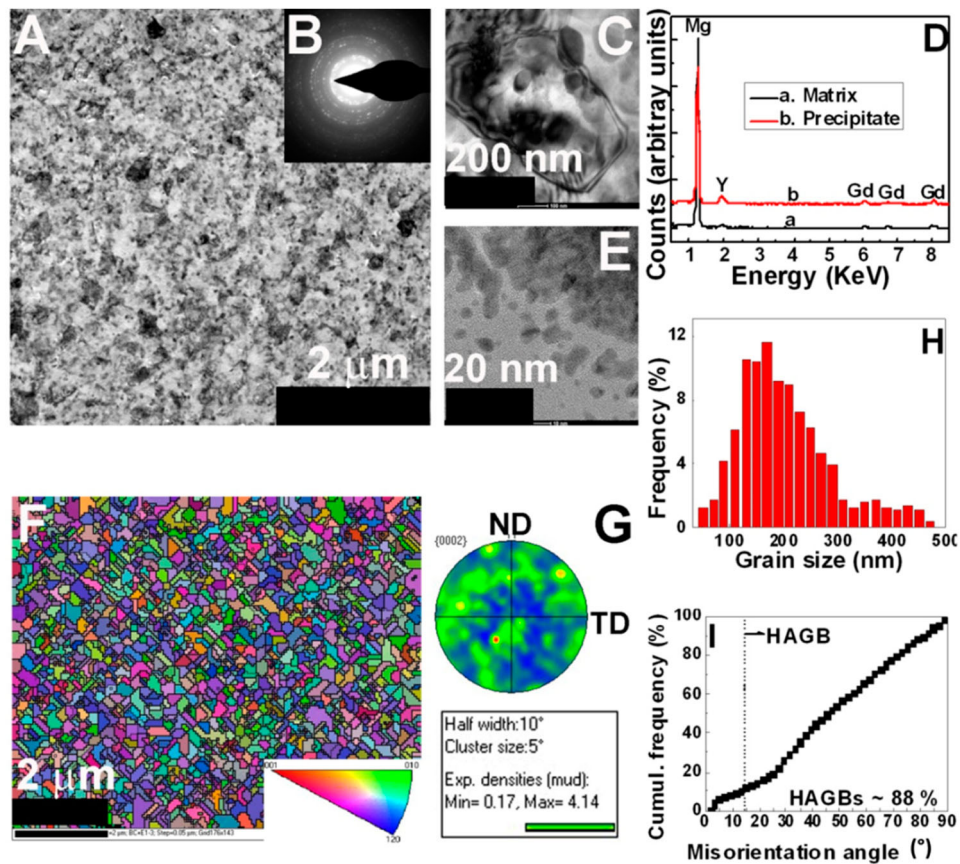

Figure 1. (A) A bright-field TEM image, (B) a selected area diffraction pattern from a 2 μm diameter area, (C) HRTEM image showing presence of coarse and ultrafine intermetallic compounds along the grain boundaries and grain interiors, (D) Chemical information about intermetallic compounds obtained by EDAX analysis, (E) HRTEM image showing presence of nano-precipitates at grain interiors, (F) IPF map, (G) Basal plane (0002) pole figure with its intensity distribution, (H) Statistical grain size distribution and (I) Misorientation angle distribution of the presently developed UFG E675 alloy.
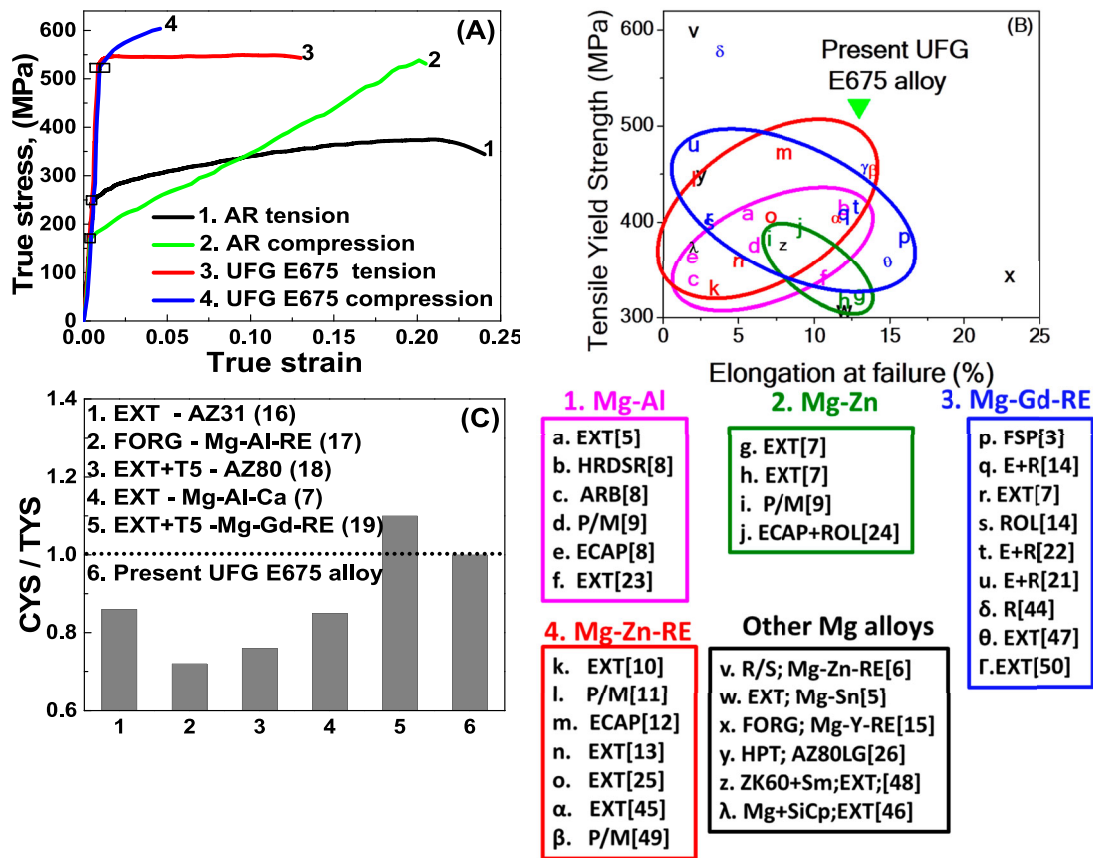
Figure 2. (A) True tensile and compressive stress-strain curves of as-received and UFG E675 alloy. (B) Comparison of tensile yield strength vs. ductility of reported high strength Mg alloys processed by various methods with the present study (EXT: Extruded, P/M: Powder Metallurgy, ECAP: Equal Channel Angular Pressed, HRDSR: High-Ratio Differential Speed Rolled, ARB: Accumulative Roll Bonded, ROL: Rolled, E + R: Extruded + Rolled, FORG: Forged, R/S: Rapidly Solidified, HPT: High-Pressure Torsion). (C) Comparison of CYS/TYS ratio of reported Mg alloys processed various techniques with the present work.

in Y and Gd. Along with RE rich intermetallic particles, a lot of spherical and plate-shape precipitates finer than 30 nm are homogeneously distributed throughout the microstructure (Figure 1(E)) which are predominantly metastable β'' and β' phases. The EBSD inverse pole figure (IPF) map also shows twin-free dynamically recrystallized equiaxed UFG (Figure 1(F)). The presence of multiple colored grains in the IPF map indicates that the orientation distribution in the UFG E675 alloy is nearly random. The basal plane (0002) pole figure (Figure 1(G)) also confirms this. The FSP Mg alloys often show strong basal texture. The lower texture intensity observed in the present UFG E675 alloy is likely to be because of the presence of fine Mg-Gd-Y along the grain boundaries which prevents the growth and alignment of recrystallized grains during FSP by pinning the grain boundaries. Black lines in Figure 1(F) show the high angle grain boundaries (HAGBs). As per grain distribution plot (Figure 1(G)), majority of the grains are below 300 nm with a mean grain size of 210 ± 120 nm. Most

of the grain boundaries have high misorientation angle (HAGB fraction is $\sim$ 88%) as shown in Figure 1(I).

3.2. Mechanical properties

Tensile and compressive tests were carried out on as-received and UFG E675 alloy samples to obtain the mechanical properties (Figure 2(A)). The yield strength (YS), ultimate tensile strength (UTS) and elongation to failure (ELON) of UFG E675 alloy are 521 and 538 MPa and 13%, respectively. As compared to the as-received sample, the UFG E675 alloy showed 230% and 170% improvement in YS and UTS, respectively. The strength properties of UFG E675 alloy are significantly higher than the best commercial wrought Mg alloys (200–300 MPa) [5]. Various conventional and severe plastic deformation (SPD) techniques were used in recent years to develop high strength Mg alloys. Figure 2(B) shows a comparison of YS vs. ELON of various high strength Mg alloys [6–15,21–26,44–50] processed by different conventional

and SPD techniques with UFG E675 alloy. The YS-ELON combination obtained for UFG E675 alloy (Figure 2(B)) is highest among all the Mg alloys produced by any technique. Furthermore, the YS and ELON of UFG E675 alloy are even superior than that of T8 treated high strength Al 2024 alloy (YS: 450 MPa and ELON: 6%) [8] and T6 treated high strength Al 7075 alloy (YS: 503 MPa, ELON: 11%) [51]. Both of these Al alloys are very popular and used for aerospace and structural applications. On the basis of microstructural features (Figure 1), the extraordinary strength in UFG E675 alloy is attributed to the combined effect of significant grain refinement ($\sim$ 200 nm), precipitation strengthening ($\sim$ 30 nm) by homogeneously distribution of nano-sized spherical and plate-shaped β'' and β'' precipitates and dispersion strengthening by fine Mg-Y-Gd rich intermetallic compounds ($\sim$ 100 nm). Along with high strength, ELON of UFG E675 alloy is also higher than most of the reported Mg alloys (Figure 2(B)). The contributing factors for effective enhancement of elongation to failure (ELON) are (i) texture randomization, (ii) presence of extremely smaller grains and (iii) random grain orientation. The 1st factor, texture randomization, is a signature for achieving enhanced formability and improved elongation to failure. The presence of RE elements (Yttrium (Y) and Gadolinium (Gd)) and the multi-pass FSP route played a major role on texture randomization. The present UFG E675 alloy contains high fraction (13 wt. %) of RE elements (Y: 6 wt. % and Gd: 7 wt. %) with high solubility limit of both Y and Gd in Mg matrix. Due to presence of high fraction of RE elements with high solubility limit: (1) the stacking fault energy of Mg matrix is affected or alters which leads to enhanced activity of $< c + a >$ non-basal slip and results in texture weakening, and (2) the Y and Gd solute atoms and Mg-Y-Gd rich intermetallic phases segregate at grain boundaries and hence restricts the grain boundary mobility via solute drag and Zener pinning effects. The restricted action for the mobility of grain boundaries allows the grains to grow in different orientation during two-pass FSP induced dynamic recrystallization which leads to texture randomization or weakening. The second factor (ii) is slip induced grain boundary sliding/accommodation due to the presence of extremely smaller grains leading to higher ELON in UFG E675 alloy. The third factor (iii) random grain orientation (Figure 1(F)) enabled multiple slip systems which resulted in enhanced ELON.

The tensile yield stress (TYS) of the as-received samples (251 MPa) is observed to be significantly higher than the compressive yield stress (CYS) (170 MPa). However, in UFG E675 alloy both tensile and compression test values are similar (TYS: 521 MPa, CYS: 522 MPa). Figure 2(C) shows the yield asymmetry of various Mg alloys processed by different techniques in comparison with UFG E675 alloy [7,16–19]. The ratio of CYS to TYS was selected as a measure of yield asymmetry in the present work. The yield asymmetry of Mg alloys processed by various SPD techniques lies in the range of 0.3–0.8 (Figure 2(C)). Such an asymmetry restricts the structural application of Mg alloys, especially for components subjected to cyclic loading. However, in the present UFG E675 alloy, the yield asymmetry is completely eliminated. Generally, yield asymmetry phenomenon is related to deformation-twinning and its magnitude could be reduced via suppression of twinning activity. Twinning is generally observed in coarse-grained Mg and its alloys which acts as an additional deformation mechanism to basal dislocation slip at room temperature in order to satisfy the von-Mises criterion [15] and hence the as-received material in the present work with an average grain size of 25 μm shows a comparatively lower CYS/TYS ratio. The Hall-Petch slope for twinning (k_{twin}) is generally larger than that for slip (k_{slip}) in case of UFG Mg alloys [16] which indicates that twinning stress has higher grain size dependence than the stress required for activation of slip. Since, in the present work, the grain size of UFG E675 alloy is extremely small ($\sim$ 200 nm), the difficulty in twinning and activation of non-basal slip (to satisfy the von-Mises criterion [16]) are likely to be the main reasons for elimination of the tensile/compression yield asymmetry. In addition to this, the presence of nano-precipitates and fine Mg-Y-Gd rich intermetallic compounds in the UFG E675 alloy creates difficulty in twin boundary migration during compression testing which acts as a possible reason in elimination/reduction of the tensile/compression yield asymmetry.

Figure 3 summarizes the specific strength (UTS/ Density) of conventional structural alloys together with the present UFG E675 alloy. The specific strength of the various metals such as Steels, Aluminium and Titanium are obtained from the standard data sheets [52,53]. It is observed that the specific strength of the present UFG E675 alloy is significantly higher than the other conventional structural alloys.

3.3. High strain rate superplasticity

In order to study the HSRS of the present UFG E675 alloy, tensile tests were carried out at temperatures ranging from 375 to 475°C at a constant strain rate of 5×10^{-2} s^{-1} and shown in Figure 4(A). The comparative study of HSRS (5×10^{-2} s^{-1}) of different types of Mg alloys processed by various conventional and SPD routes are shown in Figure 4(B) [32–43]. The HSRS (5×10^{-2} s^{-1}) of the present UFG E675 alloy exhibits $\sim$ 1300%, which
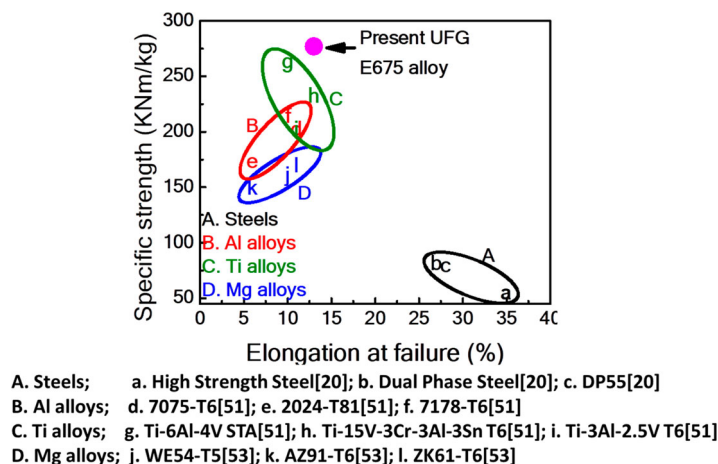
Figure 3. Specific strength of different conventional structural magnesium alloys in comparison with present UFG E675 alloy.
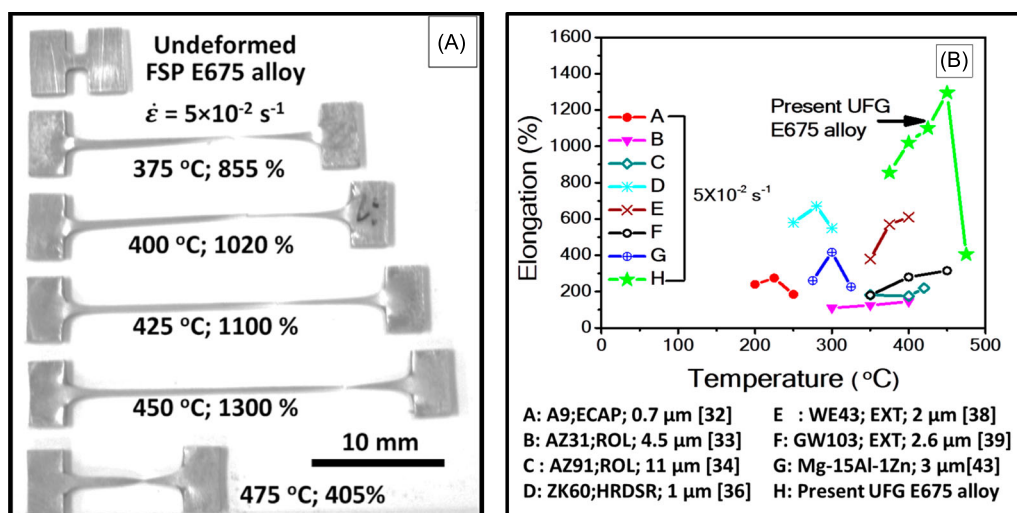

Figure 4. (A) Tensile specimens pulled to failure at different temperatures with a strain rate of 5×10^{-2} s^{-1}; (B) Comparison of HSRS properties of different reported Mg alloys processed by various routes with the present work.

is highest among all the reported Mg alloys processed by any other technique (at 5×10^{-2} s^{-1}) (Figure 4(B)).

The possible mechanism for achieving extraordinary HSRS of the present UFG E675 alloy is explained as: (i) the presence of extremely small grain size (~ 200 nm) in the present UFG E675 alloy leads to HSRS via grain boundary sliding mode, (ii) the Mg alloys should preferably deform at a temperature range of 300-500°C ($\geq$ 0.5 T_m) by multiple slip accommodation mechanisms to achieve HSRS above 1000%. But the thermal stability of most of the fine-grained Mg alloys (AZ91, ZA82, ZK60, etc.) are poor in this temperature range due to the absence of thermally stable pinning particles, resulting in lower HSRS. However, the presence of a significant fraction of heat-resistant (~ 500°C) ultrafine pinning particles along the grain boundaries in UFG E675 alloy retards the grain

growth [27] during superplastic deformation which leads to higher HSRS. One more additional contributing factor for the high thermal stability of grains at elevated superplastic temperatures is due to grain boundary segregation of RE solute atoms (Gd) which is termed as solute drag effect. As Gd has the highest tendency of solute segregation towards the grain boundaries due to its large atomic misfit percentage with Mg matrix [54]. Another distinguishing factor is the presence of high fraction of low angle grain boundaries in Mg alloys processed by various conventional and SPD routes. The existence of low angle grain boundaries in Mg alloys often retards the HSRS due to the inability of low angle or special boundaries to exhibit GBS. By comparison, the present FSPed UFG E675 alloys have a complete recrystallized microstructure with more than 88% HAGB, significantly higher

than that obtained by other conventional and SPD processing routes. Therefore, the present FSPed UFG E675 alloy exhibited highest HSRS among all other differently processed Mg alloys.

4. Summary

In short, we developed a wrought Mg-RE alloy microstructure with negligible tension-compression symmetry, high specific strength, highest combination of strength-ductility and excellent HSRS among all the existing Mg alloys reported in the literature till today. The achievement of extraordinary structural efficiency in the present Mg-RE alloy is obtained by using a two-step procedure, developing UFG Mg-RE alloys with a high fraction of high angle grain boundaries by multipass friction stir processing and employing nano-precipitates and thermally stable ultrafine intermetallic compounds to UFG Mg-RE alloy. This processing strategy may be easily adapted to many other RE contained Mg alloys to achieve exceptional structural efficiency.

Acknowledgements

Disclosure statement

Funding

ORCID

R. S. Mishra http://orcid.org/0000-0002-1699-0614

References

[1] Pollock T. Weight loss with magnesium alloys. Science. 2010;328:986–987.

[2] Gupta M, Sharon N. Magnesium, magnesium alloys, and magnesium composites. 1st ed. Hoboken (NJ): Wiley; 2011.

[3] Xiao BL, Yang Q, Yang J, et al. Enhanced mechanical properties of Mg–Gd–Y–Zr casting via friction stir processing. J Alloys Compd. 2011;509:2879–2884.

[4] He SM, Zeng XQ, Peng LM, et al. Microstructure and strengthening mechanism of high strength Mg-10Gd-2Y-0.5Zr alloy. J Alloys Compd. 2007;427:316–323.

[5] Hono K, Mendis CL, Sasaki TT, et al. Towards the development of heat-treatable high-strength wrought Mg alloys. Scr Mater. 2010;63:710–715.

[6] Innou A, Kawamura Y, Matsushita M, et al. Novel hexagonal structure and ultrahigh strength of magnesium solid solution in the Mg–Zn–Y system. J Mater Res. 2001;16:1984.

[7] Xu SW, Oh-Ishi K, Kamado S, et al. High-strength extruded Mg-Al-Ca-Mn alloy. Scr Mater. 2011;65:269–272.

[8] Kim WJ, Jeong HG, Jeong HT. Achieving high strength and high ductility in magnesium alloys using severe plastic deformation combined with low-temperature aging. Scr Mater. 2009;61:1040–1043.

[9] Kubota K, Mabuchi KH M. Processing and mechanical properties of fine-grained magnesium alloys. J Mater Sci. 1999;4:2255–2262.

[10] Singh A, Osawa Y, Somekawa H, et al. Ultra-fine grain size and isotropic very high strength by direct extrusion of chill-cast Mg-Zn-Y alloys containing quasicrystal phase. Scr Mater. 2011;64:661–664.

[11] Mora E, Garces G, Onorbe E, et al. High-strength Mg-Zn-Y alloys produced by powder metallurgy. Scr Mater. 2009;60:776–779.

[12] Chen B, Lin D, Zeng X, et al. Microstructure and mechanical properties of ultrafine grained Mg97Y2Zn1 alloy processed by equal channel angular pressing. J Alloys Compd. 2007;440:94–100.

[13] Yu W, Liu Z, He H, et al. Microstructure and mechanical properties of ZK60-Yb magnesium alloys. Mater Sci Eng A. 2008;478:101–107.

[14] Li RG, Nie JF, Huang GJ, et al. Development of high-strength magnesium alloys via combined processes of extrusion, rolling and ageing. Scr Mater. 2011;64:950–953.

[15] Panigrahi SK, Yuan W, Mishra RS, et al. A study on the combined effect of forging and aging in Mg–Y–RE alloy. Mater Sci Eng A. 2011;530:28–35.

[16] Yin DL, Wang JT, Liu JQ, et al. On tension-compression yield asymmetry in an extruded Mg-3Al-1Zn alloy. J Alloys Compd. 2009;478:789–795.

[17] Hakamada M, Watazu A, Saito N, et al. Tension/compression anisotropy in hot forged Mg-Al-Ca-RE Alloy. Mater Trans. 2009;50:1898–1901.

[18] Lv C, Liu T, Liu D, et al. Effect of heat treatment on tension-compression yield asymmetry of AZ80 magnesium alloy. Mater Des. 2012;33:529–533.

[19] Homma T, Kunito N, Kamado S. Fabrication of extraordinary high-strength magnesium alloy by hot extrusion. Scr Mater. 2009;61:644–647.

[20] Mukai T, Yamanoi M, Watanabe H, et al. Ductility enhancement in AZ31 magnesium alloy by controlling its grain structure. Scr Mater. 2001;45:89–94.

[21] Yu Z, Huang Y, Qiu X, et al. Fabrication of a high strength Mg-11Gd-4.5Y-1Nd-1.5Zn-0.5Zr (wt%) alloy by thermomechanical treatments. Mater Sci Eng A. 2015;622:121–130.

[22] Xu C, Zheng M, Xu S, et al. Improving strength and ductility of Mg-Gd-Y-Zn-Zr alloy simultaneously via

extrusion, hot rolling and ageing. Mater Sci Eng A. 2015;643:137–141.

[23] Bu F, Yang Q, Qiu X, et al. Study on the assemblage of Y and Gd on microstructure and mechanical properties of hot extruded Mg-Al-Zn alloy. Mater Sci Eng A. 2015;639:198–207.

[24] Yuan Y, Ma A, Gou X, et al. Superior mechanical properties of ZK60 mg alloy processed by equal channel angular pressing and rolling. Mater Sci Eng A. 2015;630:45–50.

[25] Liu L, Chen X, Pan F, et al. A new high-strength Mg-Zn-Ce-Y-Zr magnesium alloy. J Alloys Compd. 2016;688:537–541.

[26] Dobatkin SV, Rokhlin LL, Lukyanova EA, et al. Structure and mechanical properties of the Mg-Y-Gd-Zr alloy after high pressure torsion. Mater Sci Eng A. 2016;667:217–223.

[27] Khan MD F, Panigrahi SK. Achieving excellent thermal stability and very high activation energy in ultrafine-grained magnesium silver rare earth alloy prepared by friction stir processing. Mater Sci Eng A. 2016;675:338–344.

[28] Khan MD F, Panigrahi SK. Age hardening, fracture behavior and mechanical properties of QE22 Mg alloy. J Magnes Alloy. 2015;3:210–217.

[29] Sahoo BN, Panigrahi SK. Synthesis, characterization and mechanical properties of in-situ (TiC-TiB2) reinforced magnesium matrix composite. Mater Des. 2016;109:300–313.

[30] McFadden SX, Mishra RS, Valiev RZ, et al. Low-temperature superplasticity in nanostructured nickel and metal alloys. Nature. 1999;398:684–686.

[31] Mukherjee AK, Mishra RS, Bieler TR. Some critical aspects of high strain rate superplasticity. Mater Sci Forum. 1997;233-234:217–234.

[32] Matsubara K, Miyahara Y, Horita Z, et al. Developing superplasticity in a magnesium alloy through a combination of extrusion and ECAP. Acta Mater. 2003;51:3073–3084.

[33] Yin DL, Zhang KF, Wang GF, et al. Superplasticity and cavitation in AZ31 Mg alloy at elevated temperatures. Mater Lett. 2005;59:1714–1718.

[34] Wei YH, Wang QD, Zhu YP, et al. Superplasticity and grain boundary sliding in rolled AZ91 magnesium alloy at high strain rates. Mater Sci Eng A. 2003;360:107–115.

[35] Yan K, Sun YS, Bai J, et al. Microstructure and mechanical properties of ZA62 Mg alloy by equal-channel angular pressing. Mater Sci Eng A. 2011;528:1149–1153.

[36] Kim WJ, Lee BH, Lee JB, et al. Synthesis of high-strain-rate superplastic magnesium alloy sheets using a high-ratio differential speed rolling technique. Scr Mater. 2010;63:772–775.

[37] Yang Q, Xiao BL, Ma ZY, et al. Achieving high strain rate superplasticity in Mg–Zn–Y–Zr alloy produced by friction stir processing. Scr Mater. 2011;65:335–338.

[38] Watanabe H, Mukai T, Ishikawa K, et al. Superplasticity of a particle-strengthened WE43 Mg alloy. Mater Trans. 2001;42:157–162.

[39] Liu XB, Chen RS, Han EH. Effects of ageing treatment on microstructures and properties of Mg–Gd–Y–Zr alloys with and without Zn additions. J Alloys Compd. 2008;465:232–238.

[40] Al-Zubaydi ASJ, Zhilyaev AP, Wang SC, et al. Superplastic behaviour of AZ91 magnesium alloy processed by high-pressure torsion. Mater Sci Eng A. 2015;637:1–11.

[41] Luo ZA, Xie GM, Ma ZY, et al. Effect of yttrium addition on microstructural characteristics and superplastic behavior of friction stir processed ZK60 alloy. J Mater Sci Technol. 2013;29:1116–1122.

[42] Torbati-Sarraf SA, Langdon TG. Properties of a ZK60 magnesium alloy processed by high-pressure torsion. J Alloys Compd. 2014;613:357–363.

[43] Lee SW, Chen YL, Wang HY, et al. On mechanical properties and superplasticity of Mg-15Al-1Zn alloys processed by reciprocating extrusion. Mater Sci Eng A. 2007;464:76–84.

[44] Jian WW, Cheng GM, Xu WZ, et al. Ultrastrong Mg alloy via nano-spaced stacking faults. Mater Res Lett. 2013;1:61–66.

[45] Singh A. Tailoring microstructure of Mg-Zn-Y alloys with quasicrystal and related phases for high mechanical strength. Sci Technol Adv Mater. 2014;15:1–16.

[46] Sun XF, Wang CJ, Deng KK, et al. High strength SiCp/AZ91 composite assisted by dynamic precipitated Mg17Al12phase. J Alloys Compd. 2018;732:328–335.

[47] Gao Z, Hu L, Li J, et al. Achieving high strength and good ductility in as-extruded Mg–Gd–Y–Zn alloys by Ce micro-alloying. Materials (Basel). 2018;11(102):1–12.

[48] Guan K, Li B, Yang Q, et al. Effects of 1.5 wt% samarium (Sm) addition on microstructures and tensile properties of a Mg−6.0Zn−0.5Zr alloy. J Alloys Compd. 2018;735:1737–1749.

[49] Medina J, Pérez P, Garcés G, et al. High-strength Mg-6Zn-1Y-1Ca (wt%) alloy containing quasicrystalline I-phase processed by a powder metallurgy route. Mater Sci Eng A. 2018;715:92–100.

[50] Xu C, Fan GH, Nakata T, et al. Deformation behavior of ultra-strong and ductile Mg-Gd-Y-Zn-Zr alloy with bimodal microstructure. Metall Mater Trans A. 2018;49:1931–1947.

[51] ASM Aerospace Specification Metals, Inc., www.aerospacemetals.com.

[52] Yang Q, Guan K, Bu F, et al. Microstructures and tensile properties of a high-strength die-cast Mg–4Al–2RE–2Ca–0.3Mn alloy. Mater Charact. 2016;113:180–188.

[53] Magnesium Elektron Database. www.luxfermeltechnologies.com.

[54] Robson JD. Effect of rare-earth additions on the texture of wrought magnesium alloys: the role of grain boundary segregation. Metall Mater Trans A. 2014;45:3205–3212.